

The Casimir Effect for Fermions in One Dimension

P. Sundberg* and R.L. Jaffe†

*Center for Theoretical Physics
Department of Physics and Laboratory for Nuclear Science
Massachusetts Institute of Technology
Cambridge, Massachusetts 02139*

MIT-CTP-3406

Abstract

We study the Casimir problem for a fermion coupled to a static background field in one space dimension. We examine the relationship between interactions and boundary conditions for the Dirac field. In the limit that the background becomes concentrated at a point (a “Dirac spike”) and couples strongly, it implements a confining boundary condition. We compute the Casimir energy for a masslike background and show that it is finite for a stepwise continuous background field. However the total Casimir energy diverges for the Dirac spike. The divergence cannot be removed by standard renormalization methods. We compute the Casimir energy density of configurations where the background field consists of one or two sharp spikes and show that the energy density is finite except at the spikes. Finally we define and compute an interaction energy density and the force between two Dirac spikes as a function of the strength and separation of the spikes.

1 Introduction

When a quantum field is coupled to matter, the spectrum of its quantum fluctuations changes. The resulting energies, forces, and pressures are known in general as Casimir effects and have a variety of experimental consequences.[1, 2] In many applications the details of the coupling to materials can be idealized by boundary conditions, and the results depend on the geometry and the boundary condition alone. The Casimir

*Email: sundberg@mit.edu

†Email: jaffe@lns.mit.edu

force between grounded metal plates has now been measured quite accurately and agrees with Casimir's original prediction [2].

In Refs. [3, 4] new methods were developed to examine Casimir effects without resorting to boundary conditions *ab initio*. Instead the fluctuating fields are coupled to a non-dynamical background field, the renormalized effective energy is calculated using standard methods of quantum field theory and renormalization theory, and examined in the limit that the background becomes sharp and strong enough to enforce a boundary condition on the fluctuating fields [5]. In general the renormalized effective energy diverges in this limit, indicating that the physical situation depends in detail on the coupling between the field and the matter. In the examples studied in Refs. [3, 4] forces between rigid objects and energy densities away from boundaries remain finite and agree with the boundary condition idealization. However the Casimir pressure on an isolated surface was found to diverge in the boundary condition limit, signalling that it depends in detail on the properties of the material that provide the physical ultraviolet cutoff.[6]

In this paper we apply the methods of Refs. [3, 4] to fluctuating Dirac fermions in one dimension. Fermionic Casimir effects are interesting in their own right, for example in the bag model of hadrons.[7, 8] Boundary conditions are in general more disruptive to Dirac fields than boson fields because the equations of motion are first order, so we anticipate that fermion Casimir effects will provide an instructive laboratory to study the difference between the approach of Refs. [3, 4] and the boundary condition method.

Our object is to treat the boundary condition as the limiting form of the coupling to a smooth, finite background potential, $\mathcal{L}_{\text{int}} = \lambda \bar{\psi} V(x) \psi$. We concentrate on potentials, $V(x)$, that couple like the mass, because such backgrounds lead to a confining (bag) boundary condition when they become strong.[7] As in the scalar case, the boundary condition limit is achieved by letting $V(x)$ become concentrated at one point (the “sharp” limit) – we refer to this standard configuration as a “Dirac spike” – and then letting $\lambda \rightarrow \infty$ (the “strong” limit). In the Dirac case the renormalized vacuum fluctuation energy diverges already in the sharp limit. In the boson case it was finite for a sharp background in one dimension and diverged only in the limit $\lambda \rightarrow \infty$. Our results on the energy density and the force between “Dirac spikes” are more positive. We find that the renormalized vacuum fluctuation energy density away from the spikes is finite even in the strong limit, and that the force between Dirac spikes is also finite.

In Section 2 we discuss the behavior of the Dirac equation in the presence of an interaction concentrated at a single point. We show that it is most convenient to represent the interaction by a transfer matrix which relates the Dirac wavefunction on the immediate left of a singularity to the wavefunction on the immediate right. In this way we are able to define the Dirac spike which is the subject of much of the rest of our work and which implements a bag boundary condition in the limit $\lambda \rightarrow \infty$.

In Section 3 we briefly review the method developed in Ref. [9] to compute the

total renormalized Casimir energy in a background field. We emphasize that the divergences that appear in the case of a smooth background are cancelled by allowed counterterms already present in the continuum Lagrangian. We then apply this formalism to compute the energy associated with a single Dirac spike, and find that it is ill defined.

In Section 4 we consider energy densities and forces between Dirac spikes. First we introduce a method based on the Greens function[4], which allows us to compute the energy density outside the region of interaction. We then apply this method to compute the energy densities of configurations with one Dirac spike at the origin, and two spikes separated by a distance d , both of which we find to be finite even as $\lambda \rightarrow \infty$. We then introduce an interaction energy density, defined as the energy density of the two spike configuration minus twice the energy density of a single spike, placed to cancel the local divergences in the energy density, and conclude by integrating the interaction energy density to compute the total energy. From that we derive the force between the two Dirac spikes in one dimension.

The problem of vacuum fluctuations of the Dirac field in one dimension has been studied previously[10, 11]. In Ref. [12, 13] boundary conditions were imposed *ab initio*, and zeta function regularization was used to control divergences. In Ref. [14], zeta function regularization was used to derive an expression for the total energy of a configuration of two parallel plates, also using boundary conditions. In [15], expressions for zero-point energies and energy densities were developed using a zeta function regularization framework, but the physical potential implementing the boundary conditions was not taken into account. In this paper we implement the boundary conditions as the limit of a finite potential. In this way we can control the subtleties of the calculation at every step enabling us to confidently distinguish what is finite and cutoff independent and what is divergent in the boundary condition limit.

This work is related to Ref. [16], which applied the methods of Ref. [9] to fermion fluctuations in a smooth background in one dimension, but did not consider either the energy density or the limit of sharp and strong backgrounds necessary to implement boundary conditions. In this paper, we will adopt the renormalization conventions of Ref. [16] and refer the reader there for further discussion.

2 The Dirac Equation in a Singular Background

The equation of motion for the fluctuations of a Dirac field in a non-dynamical background field, V , in one dimension reads

$$\left[-i\alpha \frac{d}{dx} + \beta m + V(x) \right] \psi(x) = \omega \psi(x) \quad (2.1)$$

Here, $\alpha = \gamma_0 \gamma_1$, $\beta = \gamma_0$ are two-by-two matrices, and ω is the energy eigenvalue of the time-independent solution $\psi(x)$ given the potential $V(x)$. We work in a chiral

basis, $\alpha = \sigma_3$, $\beta = \sigma_1$, $\gamma_5 = \gamma_0\gamma_1 = \sigma_3$. Our spinor normalization for right- ($k > 0$) and leftgoing ($k < 0$) waves (when $V = 0$) is determined by

$$\psi_0(k, x) \equiv v(k)e^{ikx} = \begin{pmatrix} \sqrt{\omega + k} \\ \sqrt{\omega - k} \end{pmatrix} e^{ikx} \quad (2.2)$$

with $k = \sqrt{\omega^2 - m^2}$. Note that $V(x)$ is matrix-valued. In its most general form,

$$V(x) = V_0(x)I + V_1(x)\alpha + V_2(x)\beta + V_3(x)\alpha\beta, \quad (2.3)$$

where V_0 , V_1 , and V_2 are real and V_3 is imaginary. For simplicity we exclude backgrounds proportional to $\alpha\beta$. This eliminates interactions of the form $\mathcal{L}_{\text{int}} = \bar{\psi}\gamma_5 V_3(x)\psi$. In addition, V_1 can be gauged away. To show this, assume that $\psi(x)$ solves eq. (2.1) when $V_1(x) = 0$. Then it is easy to show that

$$\chi(x) = A(x)\psi(x) = e^{-i\int_0^x V_1(x')dx'}\psi(x) \quad (2.4)$$

solves eq. (2.1) for any $V_1(x)$. Since V_1 only affects the phase of the solutions (and is independent of energy), the density of states as a function of x and ω is independent of V_1 , and we conclude that the energy density and hence the total energy are independent of V_1 . We can therefore, without further loss of generality, consider only potentials that can be written as a linear combination of the identity and β . To demonstrate the physical significance of the two remaining terms, reorder the terms in eq.(2.1),

$$\left[-i\alpha \frac{d}{dx} + \beta(m + M(x)) \right] \psi(x) = (\omega - \phi(x))\psi(x). \quad (2.5)$$

where we have replaced $V_0(x)$ by $\phi(x)$ and $V_2(x)$ by $M(x)$

The component proportional to β in effect acts like an extra mass term and the component proportional to the identity acts like an electrostatic potential. The mass term affects positive and negative energy eigenstates identically, both are attracted or both repelled. The electrostatic potential, on the other hand, treats positive and negative energy eigenstates in an opposite manner, attracting one and repelling the other. A significant portion of the later discussion will be focused on the pure mass-like potential.

As explained in the Introduction, we intend to implement a boundary condition as the limit of a finite potential. We must first investigate how this can be done for the Dirac equation in a consistent way. For simplicity, whenever the explicit form of the finite potential is needed, we will use a rectangular barrier. As the barrier width a goes to zero while its area remains constant, the potential can be replaced by a transfer matrix relating ψ at the left of the barrier to ψ at the right. We call this object a ‘‘Dirac spike’’. If we then let the area under the barrier go to infinity, the domains to the left and right of the spike decouple and ψ obeys a flux conserving boundary condition at the spike. Depending on the matrix nature of the potential, the Dirac spike may have up to two bound states.

In the scalar case the representation of a pointlike potential is simple: a delta function potential serves the purpose. Since the Dirac equation is first order, however, a delta function potential leads to contradictions. For example, consider a masslike potential $V(x) = \beta M \delta(x)$. Written out in components the Dirac equation becomes

$$-i \frac{d\psi_1}{dx} + (m + M\delta(x))\psi_2 = \omega\psi_1 \quad (2.6)$$

$$i \frac{d\psi_2}{dx} + (m + M\delta(x))\psi_1 = \omega\psi_2. \quad (2.7)$$

The terms involving a delta-function are only well defined if ψ is continuous at $x = 0$. However the first equation implies a jump in ψ_1 for continuous ψ_2 , and the second requires a jump in ψ_2 for continuous ψ_1 . Thus the equations are not consistent.

Anticipating that a sharp potential will generate a discontinuity in ψ at the point of interaction, we study a sharp potential as the limit of a finite one. Consider a potential of the form

$$V(x, a) = \Gamma b(x, a), \quad (2.8)$$

where $b(x, a)$ is defined to be $1/a$ for $0 \leq x \leq a$ and 0 otherwise, and Γ is some matrix-valued constant. It is easy to show that the solution to the Dirac equation in a potential of the form of eq. (2.8) is a continuous function of x .

Since the Dirac equation is first order, $\psi(x)$ is completely determined from its value at any point. In particular, given $\psi(0)$, we can compute $\psi(a)$, $\psi(a) = T(\Gamma, a, \omega)\psi(0)$, where the two dimensional transfer matrix, T , depends on ω , a , and Γ . As long as a is finite, ψ is continuous everywhere. But as we take the limit $a \rightarrow 0$, keeping Γ fixed, ψ is no longer continuous at $x = 0$. We therefore define the transfer matrix for a Dirac spike by $T(\Gamma, \omega) = \lim_{a \rightarrow 0} T(\Gamma, a, \omega)$ with the jump condition

$$\psi(0^+) = T(\Gamma, \omega)\psi(0^-). \quad (2.9)$$

where $\psi(0^\pm) = \lim_{x \rightarrow 0^\pm} \psi(x)$.

The properties of T depend on both the strength and Dirac matrix character of Γ . As advertised we limit our discussion to potentials of the form,

$$\Gamma = \theta I + \lambda \beta, \quad (2.10)$$

where $\theta = \phi a$ and $\lambda = Ma$ are constants. For finite a we obtain

$$T(M, \phi, a, \omega) = \begin{pmatrix} \cos qa + i \frac{\omega - \phi}{q} \sin qa & -i \frac{m+M}{q} \sin qa \\ i \frac{m+M}{q} \sin qa & \cos qa - i \frac{\omega - \phi}{q} \sin qa \end{pmatrix} \quad (2.11)$$

where $q = \sqrt{(\omega - \phi)^2 - (m + M)^2}$. In the limit $a \rightarrow 0$ for any fixed value of ω , we obtain the transfer matrix for the general Dirac spike,

$$T(\lambda, \theta) = \begin{pmatrix} \cos \sqrt{\theta^2 - \lambda^2} - i \frac{\theta}{\sqrt{\theta^2 - \lambda^2}} \sin \sqrt{\theta^2 - \lambda^2} & -i \frac{\lambda}{\sqrt{\theta^2 - \lambda^2}} \sin \sqrt{\theta^2 - \lambda^2} \\ i \frac{\lambda}{\sqrt{\theta^2 - \lambda^2}} \sin \sqrt{\theta^2 - \lambda^2} & \cos \sqrt{\theta^2 - \lambda^2} + i \frac{\theta}{\sqrt{\theta^2 - \lambda^2}} \sin \sqrt{\theta^2 - \lambda^2} \end{pmatrix} \quad (2.12)$$

This is the generalization of the delta function potential to the Dirac equation (modulo our exclusion of pseudoscalar couplings). Note that in the limit $a \rightarrow 0$ T becomes independent of ω and can therefore be regarded as a background “potential” in the Dirac equation.

Two special cases are of interest. The masslike case, where $\theta = 0$, will play the principal part in the sections that follow,

$$T_M(\lambda) = \begin{pmatrix} \cosh \lambda & -i \sinh \lambda \\ i \sinh \lambda & \cosh \lambda \end{pmatrix} = e^{i\gamma_1 \lambda} \quad (2.13)$$

For completeness, we will also compute the electrostatic case, where $\lambda = 0$,

$$T_E(\theta) = \begin{pmatrix} e^{-i\theta} & 0 \\ 0 & e^{i\theta} \end{pmatrix} = e^{-i\gamma_5 \theta} \quad (2.14)$$

These two potentials may or may not have bound states. For the pure mass-like case, there are positive and negative energy bound states when $\lambda < 0$. The energy eigenvalue obeys

$$\frac{\sqrt{m^2 - \omega_M^2}}{m} \equiv \frac{\kappa_M}{m} = -\tanh \lambda, \quad (2.15)$$

whereas in the electrostatic case, there is one bound state in either the positive or negative energy spectrum regardless of the sign of θ ,

$$\frac{\sqrt{m^2 - \omega_E^2}}{\omega_E} \equiv \frac{\kappa_E}{\omega_E} = -\tan \theta \quad (2.16)$$

Equations (2.15) and (2.16) are qualitatively different. Whatever the sign of the electrostatic interaction, it is attractive either for particles (positive energy states) or antiparticles (negative energy states). The electrostatic interaction violates charge conjugation invariance so the spectrum need not be symmetric, however it is periodic in $\theta \rightarrow \theta + 2\pi$. The masslike spike has either no bound states when it is repulsive, or exactly one positive energy and one negative energy bound state when it is attractive. The energy spectrum is symmetric since a masslike interaction preserves charge conjugation invariance.

The probability current passing through a masslike spike goes to zero as the strength of the spike goes to infinity. Effectively the spike becomes a wall, splitting the line into two independent half lines. This situation is familiar from bag models, and not surprisingly the masslike spike reduces to a bag boundary condition in this limit.[7] In contrast the electrostatic spike is periodic in the strength θ and therefore does not reach a limit as $\theta \rightarrow \infty$. While this phenomenon is interesting in its own right, we do not pursue it any further here.

As $\lambda \rightarrow \infty$, eq. (2.13) becomes

$$T_M(\lambda) = e^\lambda \begin{pmatrix} 1 & -i \\ -i & 1 \end{pmatrix} + \mathcal{O}(e^{-\lambda}) \quad (2.17)$$

For $\psi(0^+)$ to be finite, it is necessary that

$$\psi_1(0^-) = i\psi_2(0^-) + \mathcal{O}(e^{-\lambda}), \quad (2.18)$$

from which it follows that

$$\psi_1(0^+) = -i\psi_2(0^+) + \mathcal{O}(e^{-\lambda}). \quad (2.19)$$

Eqs. (2.18) and (2.19) can be written as two independent boundary conditions on the half lines separated by a true boundary at $x = 0$,

$$(1 + i\gamma_1)\psi(0^+) = 0 \quad (2.20)$$

$$(1 - i\gamma_1)\psi(0^-) = 0, \quad (2.21)$$

which are standard bag boundary conditions and insure that the probability current, $j = \bar{\psi}\gamma_1\psi$ vanishes at $x = 0$.

3 Total Renormalized Vacuum Fluctuation Energy

In this section we briefly review the method developed in Ref. [9, 3] to compute the Casimir energy of a field configuration from scattering data, and adapt it to the case of a Dirac fermion in a static background in 1+1 dimensions. Our work is based on the prescription of Ref. [16], specialized to a sharply peaked background. We first review the fundamentals of the method, including how the phase shifts are related to the density of states. We then show how the resulting highly oscillating energy integrals can be evaluated using contour integration, significantly simplifying the numerical computations.

We first confront the case of a Dirac spike directly and find that it generates a divergent renormalized vacuum fluctuation energy. We then compute the total energy of a potential of the form of eq. (2.8), only afterwards taking the potential to be sharp and strong. Using this approach, the total energy is well defined for finite width, a , of the potential, but diverges as $a \rightarrow 0$ with the integral of the potential fixed.

In one dimension the S matrix can be written in terms of the transmission and reflection coefficients,

$$S = \begin{pmatrix} T & R_1 \\ R_2 & T \end{pmatrix}. \quad (3.1)$$

The transmission coefficients for right and leftgoing waves must be identical by time reversal symmetry, but the two reflection coefficients can differ. The S matrix is constrained to be unitary, $S^\dagger S = I$. In addition, as k becomes large, any finite potential becomes negligible, and we expect the S matrix to become the identity in this limit. Of course we are considering singular potentials, so this property must

be studied carefully. In a basis of eigenchannels, the S matrix is diagonal, and its eigenvalues are complex exponentials of the phase shifts,

$$S = \begin{pmatrix} e^{2i\delta_1(k)} & 0 \\ 0 & e^{2i\delta_2(k)} \end{pmatrix}. \quad (3.2)$$

The change in the density of states, $\Delta\rho(k)$, due to the interaction is related to the trace-log of S , $\Delta(k) = \frac{1}{2i}\text{Tr} \ln S(k) = \delta_1(k) + \delta_2(k)$ [9],

$$\Delta\rho(k) = \rho(k) - \rho^0(k) = \frac{1}{\pi} \frac{d\Delta(k)}{dk} = \frac{1}{2\pi i} \frac{d \ln \det S}{dk}. \quad (3.3)$$

Following Refs. [5] and [16] we write the *renormalized* Casimir energy for any non-singular background, $V(x)$, as

$$\Delta E_{\text{cas}} = - \sum_j (\omega_j - m) - \int_0^\infty dk (\omega(k) - m) \Delta\bar{\rho}(k) + \bar{\Gamma}_{\text{FD}}, \quad (3.4)$$

Note the negative sign and factor of two relative to the Casimir energy of a real scalar field. The sum is over possible bound states, and

$$\Delta\bar{\rho}(k) = \frac{1}{\pi} \frac{d}{dk} \bar{\Delta}(k) \equiv \frac{1}{\pi} \frac{d}{dk} (\Delta(k) - \Delta^{(1)}(k)), \quad (3.5)$$

where $\Delta^{(1)}(k)$ is the first Born approximation to $\Delta(k)$. The subtraction of the first Born approximation is compensated by adding back the corresponding Feynman diagrams, which are then combined with the counterterms to give the renormalized Feynman diagram contribution, $\bar{\Gamma}_{\text{FD}}$. We work in the “no tadpole” renormalization scheme where the counterterms exactly cancel the local, divergent Feynman diagrams. In this renormalization scheme $\Gamma_{\text{FD}} = 0$. For more discussion of the derivation of eq. (3.4) we refer the reader to Ref. [16].

The formalism of Ref. [5] and eq. (3.4) gives a finite renormalized energy for any finite potential. However, the total energy of a Dirac spike is infinite. This is easy to see by computing the associated shifted density of states and examining its behavior at large k .

The S matrix can easily be obtained from the transfer matrix, eq. (2.13). The result is

$$S = \begin{pmatrix} T & R_1 \\ R_2 & T \end{pmatrix} = \frac{1}{k \cosh \lambda + im \sinh \lambda} \begin{pmatrix} k & -i\omega \sinh \lambda \\ -i\omega \sinh \lambda & k \end{pmatrix}. \quad (3.6)$$

It is already apparent that the Dirac spike is a badly behaved. We expect $S \rightarrow I$ as $k \rightarrow \infty$, but instead

$$S \rightarrow \begin{pmatrix} \text{sech} \lambda & -i \tanh \lambda \\ -i \tanh \lambda & \text{sech} \lambda \end{pmatrix}.$$

Furthermore, subtraction of the first Born approximation, *ie.* of the terms linear in λ , does not suffice to render the k integral convergent. Specifically

$$\Delta\rho(k) = \frac{1}{\pi} \frac{d}{dk} \Delta(k) = \frac{1}{\pi} \frac{m \sinh \lambda \cosh \lambda}{k^2 \cosh^2 \lambda + m^2 \sinh^2 \lambda}. \quad (3.7)$$

so the integrand in eq. (3.4), $(\omega(k) - m)\Delta\bar{\rho}(k)$, is proportional to $\frac{\tanh \lambda - \lambda}{k}$ at large k , and the k integration diverges logarithmically. It would be necessary to subtract a term proportional to $\tanh \lambda$ in order to render the integral finite, and there is no justification in conventional field theory for a subtraction that includes all orders in λ . We conclude that the Casimir energy diverges for a Dirac spike, even at finite λ .

Having encountered a problem confronting the Dirac spike directly, we back off and instead compute the total renormalized Casimir energy of a finite mass barrier, and study the difficulties that develop as the potential becomes sharp. We first compute the shift in the density of states by calculating $\Delta(k) = \frac{1}{2i} \ln \det S$. The S matrix for this configuration is

$$S = \frac{1}{kq \cos qa + i(mM - k^2) \sin qa} \begin{pmatrix} kq e^{-ika} & -iM\omega \sin qa \\ -iM\omega \sin qa e^{-2ika} & kq e^{-ika} \end{pmatrix} \quad (3.8)$$

From this we conclude that

$$\begin{aligned} \frac{d}{dk} \Delta(k) = \frac{1}{2i} \frac{d}{dk} \ln \det S &= \frac{aM(k^2m + k^2M \cos^2 qa - m^2M \sin^2 qa)}{k^2q^2 + M^2\omega^2 \sin^2 qa} - \\ &\quad \frac{M^2 \sin qa \cos qa (k^2 + mM + 2m^2)}{k^2q^3 + M^2\omega^2q \sin^2 qa} \end{aligned} \quad (3.9)$$

Taking $M \rightarrow \infty, a \rightarrow 0$, with $aM = \lambda$ fixed, sends $qa \rightarrow i\lambda$, and eq. (3.9) becomes eq. (3.7), as it must. The first Born approximation is given by¹

$$\Delta^{(1)}(k) = -\frac{aM}{k} \left(m + \frac{M}{2}\right). \quad (3.10)$$

We compute the Casimir energy from eq. (3.4)

$$\begin{aligned} E_{\text{Cas}}(m, M, a) &= -\frac{1}{\pi} \int_0^\infty (\omega - m) \frac{d}{dk} (\Delta(k) - \Delta^{(1)}(k)) dk \\ &= -\frac{aM^2}{\pi} \int_0^\infty \frac{dk(\omega - m)}{k^4q^3 + k^2q\omega^2M^2 \sin^2 qa} \left(\frac{k^4q}{2} \cos 2qa \right. \\ &\quad + k^2q \left(\frac{M^2}{2} + 2mM + 2m^2 \right) - q \sin^2 qa (\omega^2 M (m + \frac{M}{2}) + m^2k^2) \\ &\quad \left. - k^2 \sin qa \cos qa (k^2 + mM + 2m^2) \right) \end{aligned} \quad (3.11)$$

It is easy to see that $E_{\text{Cas}}(m, M, a)$ is finite for finite M , as it must be, but it diverges as $\lambda M \ln \frac{M}{m}$ as $a \rightarrow 0$ with $\lambda = Ma$ fixed.

¹The first Born approximation in the Dirac theory is equal to the tadpole plus the local part of the self-energy Feynman Diagram. The explicit form can be derived by writing the Dirac equation as a second order equation and applying the general formalism.[16]

4 Greens Functions and the Energy Density

The phase shift formalism does not allow us to compute energy densities. In this section we extend the formalism of Ref. [4] based on the Greens function to enable us to study energy densities. We relate the trace of the Greens function to the *local* density of states and integrate over k to obtain the local energy density. We then construct the Greens function from solutions to the Dirac equation. We compute the free Greens function and the interacting Greens function for one and two spike potentials, and finally use the result to compute the force between two Dirac spikes.

In one dimension, the Greens function $S(x, x', \omega)$ is a 2×2 matrix, and obeys

$$(-\omega - i\alpha \frac{d}{dx} + V(x))S(x, x', \omega) = \delta(x - x') \quad (4.1)$$

We can write S as

$$S(x, x', \omega) = \sum_n \frac{\psi_n(x)\psi_n^\dagger(x')}{\omega_n - \omega - i\epsilon} \quad (4.2)$$

where

$$(-i\alpha \frac{d}{dx} + V(x))\psi_n = \omega_n \psi_n \quad (4.3)$$

and

$$\sum_n \psi_n(x)\psi_n^\dagger(x') = \begin{pmatrix} 1 & 0 \\ 0 & 1 \end{pmatrix} \delta(x - x'). \quad (4.4)$$

From eq. (4.2) we define a *local* density of states,

$$\rho(x, \omega) \equiv \frac{1}{\pi} \text{Im Tr } S(x, x, \omega) = \sum_n \delta(\omega_n - \omega) \psi_n^\dagger(x) \psi_n(x) \quad (4.5)$$

We can use the local density of states to compute the local energy density (or indeed any other local density functional of the Dirac field). To compute the energy density we integrate the density of states weighted by the energy. However, we must remember that the ground state energy for a fermion is $-\omega$, so

$$\epsilon(x) = -\frac{1}{\pi} \int_0^\infty d\omega \, \omega \text{Im Tr } \bar{S}(x, x, \omega) = -\frac{1}{\pi} \int_0^\infty dk \, k \text{Im Tr } \bar{S}(x, x, \omega(k)) \quad (4.6)$$

where $\bar{S}(x, x', \omega) \equiv S(x, x', \omega) - S_0(x, x', \omega)$, where S_0 is the free Greens function.

The free Greens function S_0 is given by

$$S_0(x, x', \omega) = \frac{i\omega}{k} \left\{ \theta(x' - x) v(-k) v^\dagger(k) \beta e^{ik(x' - x)} + \theta(x - x') v(k) v^\dagger(-k) \beta e^{ik(x - x')} \right\}. \quad (4.7)$$

where $v(k)$ is the free Dirac spinor defined by eq. (2.2). For a configuration with one spike, the Greens function is

$$S_1(x, x', \omega) = S_0(x, x', \omega) + \frac{\omega^2}{k} \frac{\sinh \lambda}{k \cosh \lambda + im \sinh \lambda} v(k) v^\dagger(k) \beta e^{ik(x+x')} \quad (4.8)$$

and for a configuration with two spikes located at $x = \pm d/2$ it becomes

$$\begin{aligned} S_2(x, x', \omega) = & S_0(x, x', \omega) - \frac{i\omega^3}{k^3} T_2(\omega) \sinh^2 \lambda e^{2ikd} \times \\ & \left(v(k) v^\dagger(-k) \beta e^{ik(x-x')} + v(-k) v^\dagger(k) \beta e^{ik(x'-x)} \right) + \\ & \frac{\omega^2}{k^2} T_2(\omega) \left(\cosh \lambda + \frac{im}{k} \sinh \lambda \right) \sinh \lambda e^{ikd} \times \\ & \left(v(k) v^\dagger(k) \beta e^{ik(x+x')} + v(-k) v^\dagger(-k) \beta e^{-ik(x+x')} \right), \end{aligned} \quad (4.9)$$

between the spikes and

$$\begin{aligned} S_2(x, x', \omega) = & S_0(x, x', \omega) + \frac{\omega^2 T_2(\omega)}{k^3} v(k) v^\dagger(k) \beta e^{ik(x+x')} \times \\ & (k \sinh 2\lambda \cos kd + 2m \sinh^2 \lambda \sin kd) \end{aligned} \quad (4.10)$$

outside the spikes. Here $T_2(\omega)$ is the transmission coefficient for the entire two-spike potential, given by

$$T_2(\omega) = \frac{k^2}{(k \cosh \lambda + im \sinh \lambda)^2 + \omega^2 \sinh^2 \lambda e^{2ikd}} \quad (4.11)$$

We combine these expressions for the Greens functions with the definition of the energy density, eq. (4.6) to obtain the energy density for the one and two Dirac spike configurations. Note that no subtractions are needed away from the spikes. The energy densities are finite, and anyway, the subtractions are local in the background field, and therefore vanish except at the spikes.

For the single spike configuration, it follows from eq. (4.8) and the symmetry under $x \rightarrow -x$ that

$$\text{Tr}\{S_1(x, x, \omega) - S_0(x, x, \omega)\} = \frac{m\omega}{k} \frac{\sinh \lambda e^{2ik|x|}}{k \cosh \lambda + im \sinh \lambda} \quad (4.12)$$

for all $x \neq 0$. Using eq. (4.6), we can now write down an expression for the energy density at $x \neq 0$,

$$\epsilon_1(x) = -\frac{1}{2\pi} \int_{-\infty}^{\infty} \text{Im} \frac{m\omega \sinh \lambda e^{2ik|x|}}{k \cosh \lambda + im \sinh \lambda} dk \quad (4.13)$$

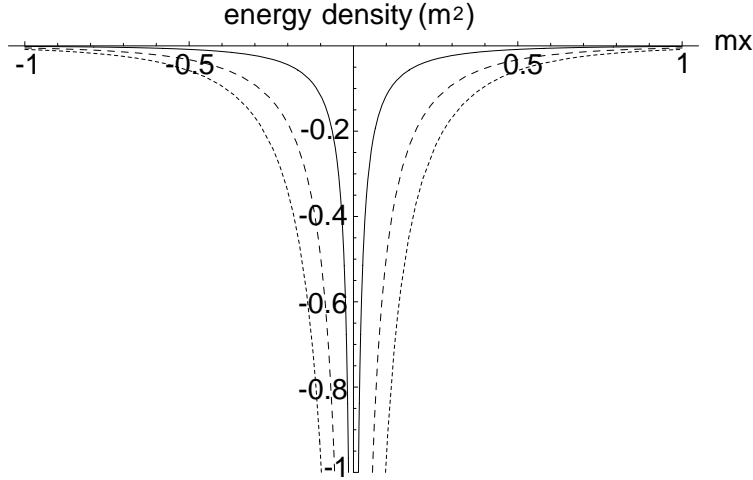


Figure 1: Energy density for configurations with a Dirac spike of strength $\lambda = 0.1$ (solid), $\lambda = 0.5$ (dashed), and as $\lambda \rightarrow \infty$ (dotted). The energy density converges uniformly as $\lambda \rightarrow \infty$.

For $x \neq 0$, the integrand of eq. (4.13) falls off exponentially in the upper half k -plane, but oscillates rapidly on the real axis. It is therefore more readily evaluated using the method of contour integration. The integrand has a branch cut on the positive imaginary axis, but no poles in the upper half plane because there are no bound states, thus

$$\epsilon_1(\xi) = -\frac{m^2}{\pi} \int_1^\infty \frac{\sqrt{\tau^2 - 1} \sinh \lambda e^{-2\tau|\xi|}}{(\tau \cosh \lambda + \sinh \lambda)} d\tau \quad (4.14)$$

where $\xi = mx$. Figure 1 shows a plot of the energy density for several choices of λ . The divergence at $x = 0$ is clearly visible for all values of λ .

As a check on this method we compute the integrated change in the density of states $\Delta\rho(k)$ by integrating $\rho(x, \omega)$ over x .

$$\Delta\rho(k) = \int_{-\infty}^\infty dx \rho(x, k) = \frac{1}{\pi} \int_{-\infty}^\infty \text{Im} \frac{m \sinh \lambda e^{2ik|x|}}{k \cosh \lambda + im \sinh \lambda} dx. \quad (4.15)$$

The integrand is even in x , so we evaluate it only for positive x , and then multiply the result by two. At the upper limit, we take $x \rightarrow \infty(1 + i\epsilon)$, and get no contribution, yielding the result

$$\Delta\rho(k) = \frac{1}{\pi} \frac{m\omega \sinh \lambda \cosh \lambda}{k^2 \cosh^2 \lambda + m^2 \sinh^2 \lambda}. \quad (4.16)$$

identical to eq. (3.7) as expected.

When we turn to two spikes, we maintain parity invariance by giving the two spikes the same strength parameter λ , and placing them at $x = \pm d/2$. The energy density is even under $x \rightarrow -x$. Hence, there are only two distinct regions: the region

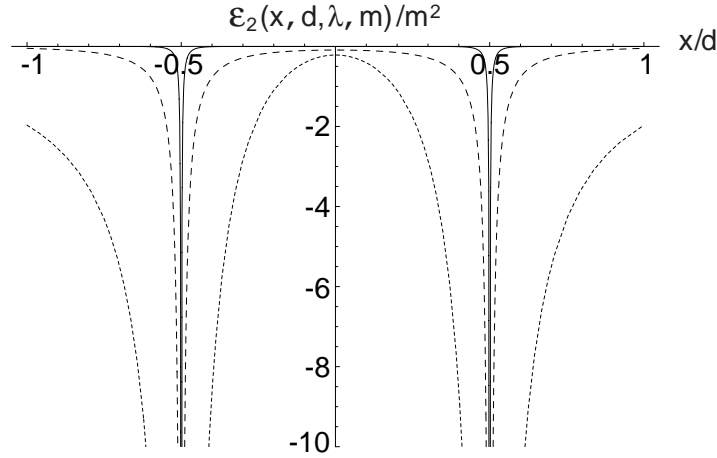


Figure 2: Energy density in units of m^2 for a configuration of Dirac spikes of strength $\lambda = 1$ of separation d , with $m = 0.1/d$ (dotted), $m = 1/d$ (dashed) and $m = 10/d$ (solid).

between the spikes, and the region outside them. Written as integrals, the energy densities are

$$\begin{aligned}
 \text{For } |x| < d/2, \quad \epsilon_2(x, d, \lambda, m) &= -\frac{1}{\pi} \int_m^\infty dt \frac{m\sqrt{t^2-m^2}(t \sinh 2\lambda + 2m \sinh^2 \lambda) e^{-td} \cosh 2t|x|}{(t \cosh \lambda + m \sinh \lambda)^2 + (t^2-m^2) \sinh^2 \lambda} e^{-2td} + \\
 &\quad \frac{2(t^2-m^2)^{3/2} \sinh^2 \lambda}{(t \cosh \lambda + m \sinh \lambda)^2 + (t^2-m^2) \sinh^2 \lambda} e^{-2td} \\
 \text{For } |x| > d/2, \quad \epsilon_2(x, d, \lambda, m) &= -\frac{1}{\pi} \int_m^\infty dt \frac{mt\sqrt{t^2-m^2} \sinh 2\lambda \cosh td}{(t \cosh \lambda + m \sinh \lambda)^2 + (t^2-m^2) \sinh^2 \lambda} e^{-2t|x|} + \\
 &\quad \frac{2m^2\sqrt{t^2-m^2} \sinh^2 \lambda \sinh td}{(t \cosh \lambda + m \sinh \lambda)^2 + (t^2-m^2) \sinh^2 \lambda} e^{-2td} \quad (4.17)
 \end{aligned}$$

The integrals converge quickly except at $x = \pm d/2$, where they diverge. A plot of the energy density for several choices of m is shown in Figure 2.

To eliminate local divergences which do not affect the force, we consider the pure interaction energy density $\bar{\epsilon}(x, d)$, defined as

$$\bar{\epsilon}(x, d) = \epsilon_2(x, d) - \epsilon_1(x - d/2) - \epsilon_1(x + d/2), \quad (4.18)$$

where $\epsilon_1(x - d/2)$ is the energy density of a single spike placed at $x = d/2$ defined in eq. (4.14). Because the divergences are local to the points of interaction, this subtraction will render the resulting expression finite everywhere. However, there is no reason to expect that the energy density should be continuous across the point of interaction, and this is indeed not the case. In particular, for $m = 0$, the energy density vanishes in the region outside the spikes, but takes a constant nonzero value in the region between them. Figures 4 and 3 show the interaction energy density in various configurations.

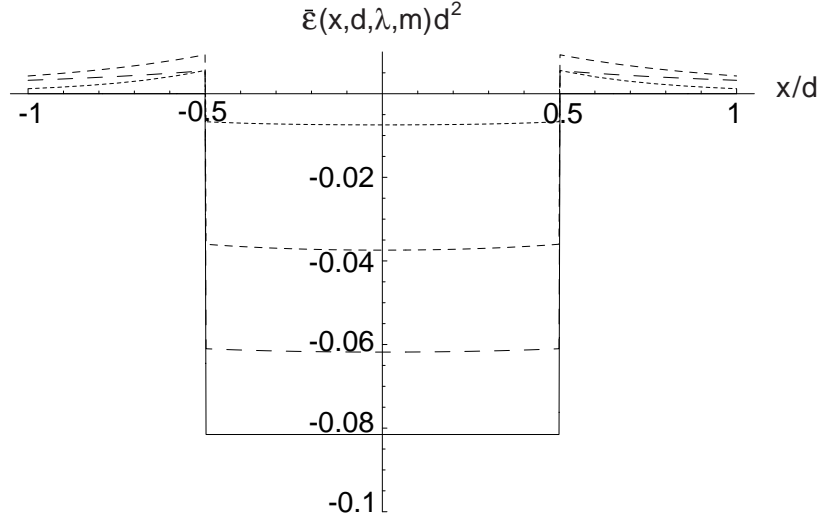


Figure 3: For small m , the interaction energy density is significant, and essentially localized between the two spikes. As m grows larger, the overall interaction term gets smaller, and energy density “leaks out” to the region outside the spikes. The plot shows $m = 0$ (solid), $m = 0.1/d$ (dashed), $m = 0.3/d$ (finely dashed), and $m = 1.0/d$ (dotted), with $\lambda = 1$ fixed.

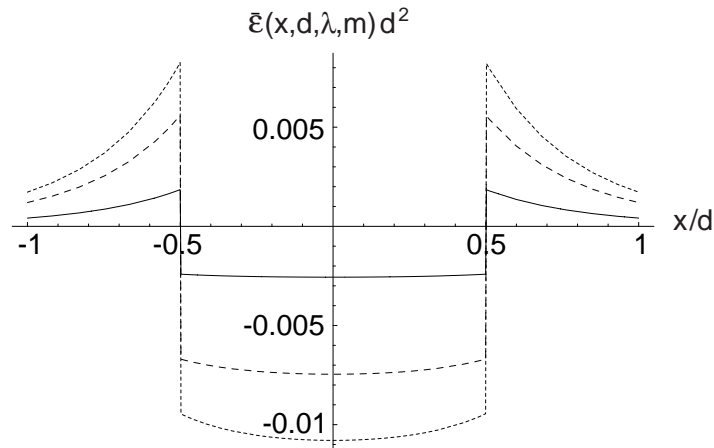


Figure 4: Interaction energy density as a function of λ . The plot shows $\lambda = 0.4$ (solid), $\lambda = 1.0$ (dashed) and $\lambda \rightarrow \infty$ (dotted), with $m = 1$ fixed. Note the discontinuities at $x = \pm d/2$.

Finally we compute the force between two spikes. Although the total Casimir energy diverges, the divergences are localized to the points of interaction and are identical to the divergences associated with a single spike. Therefore we define an “interaction Casimir energy” by subtracting away twice the contribution from a single spike from the two spike Casimir energy. The subtracted quantity is independent of d and therefore does not contribute to the force. To simplify the computation we place the centers of the two subtracted spikes at $x = \pm d/2$ respectively, and perform the subtraction within the integrand of the expression for the energy. As demonstrated in Section 4, this renders the energy density finite everywhere.

We define the total interaction energy E as the integral over x of $\bar{\epsilon}(x, d)$, defined by eq. (4.18),

$$\begin{aligned} E_{\text{int}} &= \int_{-\infty}^{\infty} dx \bar{\epsilon}(x, d) = \frac{1}{\pi} \int_m^{\infty} dt \, 2\sqrt{t^2 - m^2} \sinh^2 \lambda e^{-2td} \times \\ &\times \frac{(m^2(td + 1) - t^3d) \cosh \lambda - (md(t^2 - m^2) - mt) \sinh \lambda}{(t \cosh \lambda + m \sinh \lambda)^3 + (t^2 - m^2)(t \cosh \lambda + m \sinh \lambda) e^{-2td}} \end{aligned} \quad (4.19)$$

Since this integral is absolutely convergent, we can compute the force $F(\lambda, m, d) = -dE_{\text{int}}/dd$ by moving the derivative operator under the integral sign. The resulting expression is not very enlightening, and the t -integration must be performed numerically, however in certain interesting limits, the formula simplifies greatly.

In the limit $\lambda \rightarrow \infty$, corresponding to impenetrable spikes, or equivalently, bag boundary conditions, the total interaction energy, eq. (4.19) reduces to

$$\lim_{\lambda \rightarrow \infty} E_{\text{int}}(\lambda, m, d) \equiv E_{\text{bag}}(m, d) \quad (4.20)$$

$$= \frac{2}{\pi} \int_m^{\infty} \sqrt{t^2 - m^2} \frac{m - d(t^2 - m^2)}{t^2 - m^2 + (t + m)^2 e^{2td}} dt \quad (4.21)$$

and the force simplifies as well,

$$\lim_{\lambda \rightarrow \infty} F(\lambda, m, d) \equiv F_{\text{bag}}(m, d) \quad (4.22)$$

$$= -\frac{2}{\pi} \int_m^{\infty} \sqrt{t^2 - m^2} \frac{e^{2td}[(m^2 - t^2) + 2t^3d - 2mt(md + 1)] - (t - m)^2}{[(t - m) + (t + m)e^{2td}]^2} dt \quad (4.23)$$

These integrals can be done analytically for $m = 0$,

$$E_{\text{bag}}(0, d) = -\frac{\pi}{24d} \quad (4.24)$$

$$F_{\text{bag}}(0, d) = -\frac{\pi}{24d^2}, \quad (4.25)$$

an attractive inverse-square dependent force law.

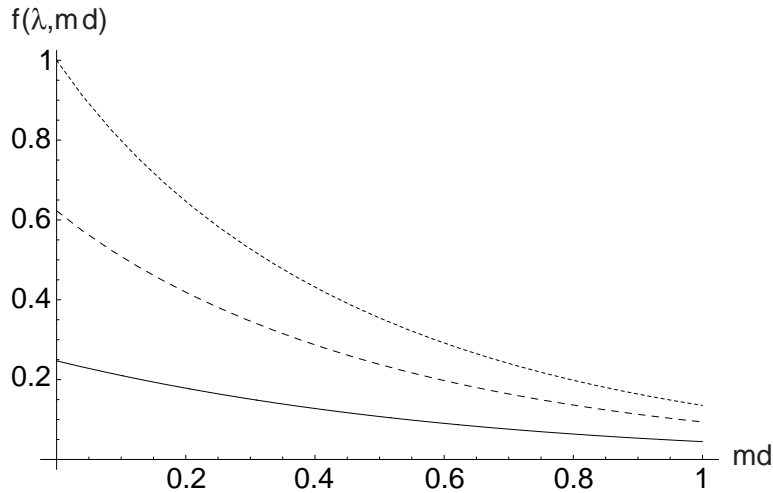


Figure 5: Force as a function of separation between the spikes. We write $F = -\frac{\pi}{24d^2}f(\lambda, md)$, and the plot shows f for $\lambda = 0.5$ (solid), $\lambda = 1$ (dashed), and $\lambda \rightarrow \infty$ (dotted).

In general, the force can be parameterized by

$$F(\lambda, m, d) = -\frac{\pi}{24d^2}f(\lambda, md), \quad (4.26)$$

where f is a dimensionless function of two dimensionless parameters and describes the departure from the force in the massless case. Figure 5 shows a plot of $f(\lambda, md)$, and Figure 6 shows $f(\lambda, 0)$. $f(\lambda, md)$ approaches a limit exponentially as $\lambda \rightarrow \infty$, $f(\lambda, 0) \sim f(\infty, 0) + C e^{-\lambda}$. As a consequence, all derivatives of f go to zero as $\lambda \rightarrow \infty$. This is visible in Figure 6.

5 Discussion

In this paper we have applied the methods of Ref. [4] to fermion fields in one dimension. The background fields were taken to be sharp spikes, imposing jump conditions on the dynamical fermion field. Using the method of computing the density of states directly from the S matrix, we showed that the total energy of such a configuration diverges and thus cannot be computed directly using the jump condition approach. The details of the interaction cannot be ignored, and the divergences introduced by a sharp potential in a fermion field are even worse than the ones that appear when the dynamical field is a scalar.

Nonetheless, energy densities and forces are still well defined. Using a formalism based on the Greens function, we showed how to compute these quantities even when the background field is highly singular, and derived expressions for the energy density

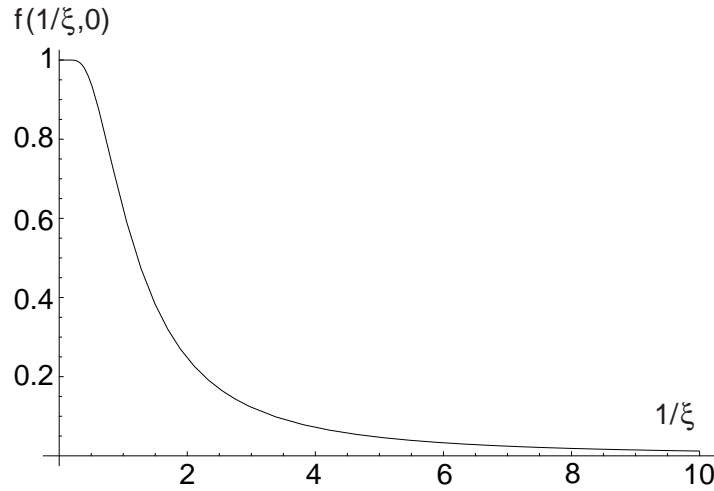


Figure 6: For $m = 0$, the force takes the form $F = -\frac{\pi}{24d^2} f(\lambda)$ for dimensional reasons. This plot shows $f(1/\xi)$ as a function of $\xi = 1/\lambda$.

in backgrounds of one and two spikes. The work culminated in a computation of the force between two spikes in the presence of a fermion field. For a massless field and spikes implementing bag boundary conditions, dimensional considerations require the force to be an inverse square force as a function of the distance between the spikes. We explicitly verified this, and computed the constant of proportionality.

6 Acknowledgements

We gratefully acknowledge discussions with V. Khemani, N. Graham, M. Quandt and E. Farhi. This work is supported in part by the U.S. Department of Energy (D.O.E.) under cooperative research agreements #DF-FC02-94ER40818.

References

- [1] H. B. Casimir, Kon. Ned. Akad. Wetensch. Proc. **51**, 793 (1948).
- [2] For a recent review, see M. Bordag, U. Mohideen and V. M. Mostepanenko, Phys. Rept. **353**, 1 (2001) [arXiv:quant-ph/0106045].
- [3] N. Graham, R. L. Jaffe, V. Khemani, M. Quandt, M. Scandurra and H. Weigel, arXiv:hep-th/0207205.
- [4] N. Graham, R. L. Jaffe, V. Khemani, M. Quandt, M. Scandurra and H. Weigel, Nucl. Phys. B **645**, 49 (2002) [arXiv:hep-th/0207120].

- [5] For a review and introduction to these methods see N. Graham, R. L. Jaffe and H. Weigel, *Int. J. Mod. Phys. A* **17**, 846 (2002) [arXiv:hep-th/0201148].
- [6] N. Graham, R. L. Jaffe, V. Khemani, M. Quandt, O. Schröder, H. Weigel, in preparation.
- [7] A. Chodos, R. L. Jaffe, K. Johnson, C. B. Thorn and V. F. Weisskopf, *Phys. Rev. D* **9**, 3471 (1974), A. Chodos, R. L. Jaffe, K. Johnson and C. B. Thorn, *Phys. Rev. D* **10**, 2599 (1974).
- [8] K. A. Milton, *Phys. Rev. D* **22**, 1441 (1980), K. A. Milton, *Phys. Rev. D* **22**, 1444 (1980)
- [9] E. Farhi, N. Graham, P. Haagensen and R. L. Jaffe, *Phys. Lett. B* **427**, 334 (1998) [arXiv:hep-th/9802015].
- [10] K. Johnson, *Acta Phys. Polon. B* **6**, 865 (1975).
- [11] K. A. Milton, *Annals Phys.* **150**, 432 (1983).
- [12] E. Elizalde, M. Bordag and K. Kirsten, *J. Phys. A* **31**, 1743 (1998) [arXiv:hep-th/9707083].
- [13] V. M. Mostepanenko and N. N. Trunov, “The Casimir Effect And Its Applications,” (Clarendon Press, Oxford, 1997).
- [14] E. Elizalde, F. C. Santos and A. C. Tort, *Int. J. Mod. Phys. A* **18**, 1761 (2003) [arXiv:hep-th/0206114].
- [15] R. D. De Paola, R. B. Rodrigues and N. F. Svaiter, *Mod. Phys. Lett. A* **14**, 2353 (1999) [arXiv:hep-th/9905039].
- [16] N. Graham and R. L. Jaffe, *Nucl. Phys. B* **549**, 516 (1999) [arXiv:hep-th/9901023].